Twisted flux tubes and how they get that way

Dana Longcope,[1] Mark Linton,[2] Alexei Pevtsov,[1] George Fisher,[2] and Isaac Klapper[3]

ABSTRACT

According to present theories, the Sun's magnetic field rises through the convection zone in the form of slender strands known as flux tubes, traditionally studied using "thin flux tube" models. While these models have been remarkably successful they have only recently begun to account for tubes with twisted magnetic flux, in spite of observational evidence for such twist. In this work we review the recent developments pertaining to twisted magnetic flux tubes and compare quantitative predictions to observations. Hydrodynamic theory predicts a role for twist in preventing fragmentation. Excessive twist can also lead to magnetohydrodynamic instability affecting the dynamics of the tube's axis. A thin tube model for a twisted tube suggests several possibilities for the origin of twist. The most successful of these is the Σ-effect whereby twist arises from deformation of the tube's axis by turbulence. Simulations show that the Σ-effect agrees with observations in magnitude as well as latitudinal dependence.

1. Flux Tubes

Magnetic field appears at the solar surface in the form of isolated domains comprising active regions (ARs). These have been understood as the manifestation of slender, pressure-confined strands of magnetic field called *flux tubes* (Parker 1955a). Flux tubes rise buoyantly as arched Ω-loops, originating at the base of the convection zone (CZ) where they are generated by dynamo action. Equations describing the dynamical evolution of a buoyant flux tube were proposed by Spruit [1981] and have been employed in modified form by subsequent investigators (Moreno-Insertis 1983; Choudhuri and Gilman 1987; Chou and Fisher 1989; D'Silva and Choudhuri 1993; Fan *et al.* 1994; Caligari *et al.* 1995; Fan and Fisher 1996). Numerical solutions of such model equations have shown good quantitative agreement with sunspot data. This agreement includes the measured "tilt angle" ψ of a

[1]Department of Physics, Montana State University

[2]Space Sciences Laboratory, UC Berkeley

[3]Department of Mathematics, Montana State University

sunspot pair as it depends on solar latitude (D'Silva and Choudhuri 1993), on magnetic flux (Fan *et al.* 1994; Fisher *et al.* 1995), and as its statistical dispersion depends on its mean (Longcope and Fisher 1996). These models fit the data with very few free parameters, and offer our best estimates of field strengths at the base of the CZ.

The model flux tube is described by its axis, a space-curve $\mathbf{x}(\ell)$, parameterized by arclength ℓ. The tube's cross section is assumed to be circle of radius $a(\ell)$ much smaller than all other scales — it is a *thin tube*. The plasma outside the tube is field-free and confines the tube by pressure ($\beta \gg 1$). Properties of the tube, such as the strength of its magnetic field $B_{\|}(\ell)$, are found from averages over the cross section: $B_{\|}(\ell) \equiv \Phi/\pi a^2(\ell)$, where Φ is the tube's total magnetic flux. The model equations describe the evolution of the axis due to magnetic tension, buoyancy and aerodynamic drag (Spruit 1981; Choudhuri and Gilman 1987). These are most often derived by truncating expansions of the fields about the axis (Ferriz-Mas and Schüssler 1990; Zhugzhda 1996), however, the same equations can be found from integration of MHD forces over a section of differential length (Longcope and Klapper 1997). Conventional derivations have assumed that the magnetic field within the tube was everywhere parallel to its axis; the tube is *untwisted*. Currents occur at the tube's boundary (a surface current) and across the axis at a bend (giving rise to a curvature force); there is no axial current $J_{\|}$.

2. The Case for Twist: Observations

Flux tubes are only truly observed where they cross the photospheric plane ($z = 0$) to form bipolar ARs. The total flux Φ is measured by integrating the vertical magnetic field, B_z, of one sign in a magnetogram (typically $\Phi = 10^{21}$ to 10^{22} Mx for an AR). The thin tube approximation is violated at the photosphere, along with several other simplifying assumptions. Nevertheless, it is frequently assumed that the tube's grossest characteristics, such as total flux and axis orientation, do not change over the top several Mm of the CZ and are therefore adequately measured at the photosphere.

Vector magnetograms often show vertical current density J_z coincident with vertical field B_z. Leka *et al.* (1996) used a sequence of vector magnetograms of emerging active region 7260 to show that the total vertical current I_z increased in concert with the total flux, in several different bipoles (each $\sim 10^{20}$ Mx). This led them to the remarkable conclusion that each flux tube was carrying axial current prior to its emergence; the flux tubes were *twisted*. In the context of the Spruit model this would correspond to an azimuthal field component B_ϕ in addition to $B_{\|}$. Since the tube is still isolated both components vanish outside the tube and there is *per force* a cancelling axial return current flowing at the tube's

surface, so that the tube carries no net current. The structure at the photosphere of such a tube, including its axial return current, is beyond any thin-tube model (there seems to be little evidence for these return currents in magnetograms (Leka *et al.* 1996)). Nevertheless, the observations of Leka *et al.* suggest that, like the total flux, the internal axial current is at most only slightly affected by this upper CZ boundary region.

Pevtsov, Canfield and Metcalf [1994, 1995] pioneered a method of quantifying the twist of an entire AR as a single value: $\alpha_{\rm pcm}$. Their technique is motivated by the constant α in a force-free field $\nabla \times \mathbf{B} = \alpha \mathbf{B}$, but does not actually assume the field to be force free (it is well known *not* to be force-free at the photosphere (Metcalf *et al.* 1995)). Measured horizontal magnetic field can be used to calculate the vertical current density $J_z(x,y) = \partial B_x/\partial y - \partial B_y/\partial x$. The ratio of current to field, J_z/B_z, can then be computed at each pixel of the magnetogram (though only where both quantities are accurately measured). Averaging this over the AR gives one global estimate of twist, $\alpha_{\rm avg}$. Alternatively, B_z can be used to compute a "force-free" version of B_x and B_y assuming a particular α. α is then varied until these vectors most closely approximate the measured values (in a least-squares sense). The minimizing value, which they call $\alpha_{\rm best}$, is a single global measurement of magnetic field twist, which we will refer to as $\alpha_{\rm pcm}$. Repeating the procedure on different magnetograms of the same AR provides one estimate of the intrinsic error in the measured value.

An extension of the original dataset to 203 ARs is shown in Figure 1 plotted against solar latitude (Longcope *et al.* 1998). The typical magnitude is $\alpha_{\rm pcm} \sim 2 \times 10^{-8}\,{\rm m}^{-1}$, comparable to calculations of $\alpha_{\rm avg}$ (Pevtsov *et al.* 1995; Leka *et al.* 1996). Substructures within an active region can have values of J_z/B_z an order of magnitude larger (Pevtsov *et al.* 1994; Leka *et al.* 1996), however, $\alpha_{\rm pcm}$ reflects the AR as a whole, and thus is the most likely to reflect the twist of the active region flux tube at depth. There is a subtle, but statistically significant, trend for $\alpha_{\rm pcm} < 0$ in the Northern hemisphere. The trend is statistically significant in the sense that the null hypothesis, that $\alpha_{\rm pcm}$ is governed by identical distributions in the two hemispheres, can be ruled out definitively. A similar equally subtle trend has been found in a large set of magnetograms analyzed in a different manner (Bao and Zhang 1998).

3. Effects of Twist: Theory

Consider a straight cylindrical flux tube with constant cross sectional radius a. If every field line in the tube has the same helical pitch $q = d\phi/d\ell$ then its field is given by

$$\mathbf{B}(r) = B_{\|}(r)\,[\,\hat{\mathbf{l}} \;+\; qr\,\hat{\phi}\,] \quad , \tag{1}$$

where $\hat{\mathbf{l}}$ and $\hat{\phi}$ are axial and azimuthal unit vectors respectively. Field lines wrap once around the axis over an axial distance $2\pi/q$. In principle the axial field profile $B_{\|}$ is arbitrary out to $r = a$, and vanishes beyond that. A simple flat profile, $B_{\|} = \Phi/\pi a^2$, has the property that $J_{\|} = 2q\,B_{\|}$. Motivated by this we will henceforth make the association $q = \frac{1}{2}\alpha_{\rm pcm}$ and note that typical observed values correspond to $q = 0.01\,\mathrm{rad/Mm}$.

3.1. Integrity

By assuming $\hat{\mathbf{l}}$ symmetry in this straightened geometry the nonlinear MHD dynamics of the cross section can be studied in two-dimensions. In the absence of twist ($q = 0$) the magnetic field behaves as a gaseous phase with partial pressure $B_{\|}^2/8\pi$ and no mass. This is analogous to a *thermal* (Turner 1973) and lacks any means of maintaining integrity (Parker 1979; Tsinganos 1980). Numerical simulations have confirmed that a two-dimensional untwisted tube will spontaneously fragment under its own buoyancy-induced motion (Schüssler 1979; Longcope *et al.* 1996).

Twist can prevent this fragmentation if the azimuthal magnetic tension is sufficient to overcome forces from the buoyant rise. A tube will rise at a terminal velocity $v_{\rm r}$ at which buoyancy is balanced by aerodynamic drag. Assuming a circular cross section, buoyancy of primarily magnetic origin and $qa \ll 1$ gives

$$v_{\rm r} \simeq \sqrt{\frac{ga|\delta\rho|}{\rho}} \simeq v_{\rm A\|}\sqrt{\frac{a}{H_{\rm p}}} \tag{2}$$

where $H_{\rm p}$ is the local pressure scale height of the external atmosphere (Parker 1975; Emonet and Moreno-Insertis 1998). In order for the azimuthal magnetic field to prevent fragmentation its Alfvén speed $v_{\rm A\perp} = qa\,v_{\rm A\|}$ must be at least as large as $v_{\rm r}$ (Tsinganos 1980). Combining these two expression gives a criterion for flux tube integrity

$$q \gtrsim \frac{1}{\sqrt{aH_{\rm p}}} \quad , \tag{3}$$

(Linton *et al.* 1996; Emonet and Moreno-Insertis 1998). This lower limit is $0.1\,\mathrm{rad/Mm}$ for the typical values $a \sim 2$ Mm and $H_{\rm p} = 50$ Mm at the base of the CZ. Nonlinear two-dimensional simulations have shown the efficacy of twist at maintaining tube integrity (Fan *et al.* 1998b; Krall *et al.* 1998), and have confirmed that expression (3) is the amount of twist required (Emonet and Moreno-Insertis 1998).

3.2. Instability

In the magnetic configuration (1) the axis is perfectly straight while the field lines are helical. Such equilibria can be susceptible to an instability, called the *helical kink*, whereby the axis spontaneously develops a helical pitch similar to that of the field lines. In low β contexts, such as fusion plasmas or the solar corona, the threshold for instability is given by a Kruskal-Shafranov criterion (Shafranov 1957; Hood and Priest 1981) $qL \gtrsim 2\pi$ where L is the axial length of the system. Infinitely long tubes are *always* unstable. In the high β pressure-confined case, however, it has been shown that instability requires

$$q \gtrsim \frac{1}{a} \quad , \tag{4}$$

even for an infinitely long tube (Linton *et al.* 1996). For an active region flux tube to be stable at the base of the CZ therefore requires $q \lesssim 0.5\,\mathrm{rad/Mm}$.

A rising flux tube which undergoes a helical kink instability will develop a bend or concentrated kink in its axis, as various unstable helical modes interact (Figure 2 (Linton *et al.* 1998a)). Nonlinear three dimensional MHD simulations have confirmed this both for a straight tube (Linton *et al.* 1998b) and a rising Ω-loop (Fan *et al.* 1998a). While the value of q will change little during the rise (see later discussion) the tube's radius a will increase dramatically. It is therefore possible for a tube to be initially stable, and become unstable during its rise (Linton *et al.* 1996).

Proper motion of emerging flux can reveal the shape of the tube's axis (Tanaka 1991; Leka *et al.* 1996). Motions of an island-δ spot analyzed by Tanaka [1991] provided evidence of a tightly knotted axis. Several of the bipolar features within AR 7260, analyzed by Leka *et al.* [1996], also exhibited a twist-like deformation. If this resulted from the helical kink mode then the axis would be deformed *in the same sense* that the field lines are twisted (in contrast to the discussion below). This was shown to be the case for each of the small bipoles within the AR. Indeed, the values of α_{avg} for each bipole was sufficient to give $qa > 1$, thus exceeding the threshold for instability. While each of the features within the AR exceed the instability threshold, the AR as a whole does not ($q\alpha_{\mathrm{avg}} \ll 1$) nor does the entire AR exhibit proper motion characteristic of a kinked axis.

4. A Model for Thin Twisted Flux Tube

Understanding the origin and evolution of twist in a flux tube requires a set of model equations applicable to general axis geometries. Several efforts have been made in this direction (Ferriz-Mas *et al.* 1989; Chui and Moffatt 1995) of which a version by

Longcope and Klapper [1997] most clearly extends the untwisted model of Spruit [1981] . As in Spruit's model the axis is a general space-curve $\mathbf{x}(\ell)$ whose local tangent vector is $\hat{\mathbf{l}}(\ell) \equiv \partial\mathbf{x}/\partial\ell$. There are two additional variables: $q(\ell)$ the field line twist, and $\omega(\ell)$ the angular velocity of internal material about $\hat{\mathbf{l}}$. An equation for the evolution of $\mathbf{x}(\ell)$ is found, exactly as in Spruit's model, by integrating the MHD forces acting on a differential tube segment (Longcope and Klapper 1997). This only changes the original Spruit equations where $q \gtrsim 1/a$. In particular, the evolution of the flux tube axis is unaffected in the *weakly twisted* limit, $qa \ll 1$. In light of the observed value $q \sim 0.01\,\mathrm{rad/Mm}$ we will henceforth consider only this limit.

The moment of the MHD forces about the axis gives an equation for the evolution of spin

$$\frac{d\omega}{dt} = v_{\mathrm{A}\|}^2 \frac{\partial q}{\partial \ell} - \frac{2}{a}\frac{da}{dt}\omega \quad . \tag{5}$$

The second term on the right hand side (rhs) leads to "spin up" in a contracting tube (due to decreasing moment of inertia). Note also that to be in equilibrium a tube must be uniformly twisted: $q(\ell) = \text{const}$. Finally, it is worth remarking that we have neglected possible torques exerted by the external fluid on the tube. If present such an effect might allow the fluid to "roll" the tube like a piece of string between two fingers (Rust 1994). Including such torques requires a model for the viscous coupling of the background to the tube's outer boundary; no such model presently exists.

While spin and twist are easily defined about a straight axis, care must be taken in their definition on a general curve $\mathbf{x}(\ell, t)$ undergoing its own time evolution. Doing so results in a kinematic relation between the two quantities (Klapper and Tabor 1994; Longcope and Klapper 1997)

$$\frac{dq}{dt} = \frac{\partial\omega}{\partial\ell} - \left(\hat{\mathbf{l}}\cdot\frac{\partial\mathbf{u}}{\partial\ell}\right) q + \hat{\mathbf{l}}\cdot\left(\frac{\partial\hat{\mathbf{l}}}{\partial\ell}\times\frac{d\hat{\mathbf{l}}}{dt}\right) \quad . \tag{6}$$

The second term on the rhs results in a decreased pitch q when the tube is stretched (the factor in parentheses is the rate of differential stretching). The first term shows the effect on twist if two portions of a tube are spinning differently; this effect is often invoked when "footpoints" are spun to impart twist. Retaining only the first rhs terms in Equations (5) and (6) leads to a wave equation for torsional Alfvén waves (Priest 1982).

The final term on the rhs of Equation (6), sometimes called the Σ-term, is the most surprising: it represents a source of twist due to the evolution of the axis alone. As a result of this term it is possible to impart twist to a section of a tube by deforming its axis in a helical manner. The sense of twist imparted turns out to be *opposite* to the sense of the axial deformation. Figure 3 shows a tube section whose axis has been given a left-handed

deformation (as if by a right-handed cyclonic event (Parker 1970)), thus causing its field lines to develop right handed twist about the axis ($q > 0$).

The necessity of the Σ-term can be appreciated in the conservation of magnetic helicity. The helicity of a closed, thin tube can be written as a sum of two terms, $H = \Phi^2(Tw + Wr)$, called *twist* and *writhe* (Berger and Field 1984; Moffatt and Ricca 1992). The individual terms are defined by the integrals

$$Tw = \frac{1}{2\pi} \oint q(\ell)\, d\ell \quad , \tag{7}$$

$$Wr = \frac{1}{4\pi} \oint d\ell \oint d\ell' \, \frac{\hat{\mathbf{l}} \times \hat{\mathbf{l}}' \cdot (\mathbf{x} - \mathbf{x}')}{|\mathbf{x} - \mathbf{x}'|^3} \quad , \tag{8}$$

where $\mathbf{x} \equiv \mathbf{x}(\ell)$, $\mathbf{x}' \equiv \mathbf{x}(\ell')$ and so on. Magnetic helicity H is strictly conserved under ideal motions and we are considering only ideal motion. Therefore, a change in writhe must be offset by an opposite change in twist. Writhe depends only on the axis while twist depends only on q, so that a deformation of the axis must be accompanied by a change in q. A left-handed helical deformation of the axis will add negatively to Wr, which will therefore cause a positive change in q, as seen in Figure 3.

5. On the Possible Origins of Twist

To find possible sources of twist in a rising tube, we may seek instead sources of writhe. For the purpose of quantifying these we will begin by assuming flux tubes to be generated in an *untwisted* and *unwrithed* state ($Tw_0 = Wr_0 = 0$). Subsequent writhing of the axis will then result in an equal and opposite twist. Twist density q is introduced by the Σ-term in Equation (6) whence it is distributed along the axis by the propagation of torsional Alfvén waves.

5.1. Joy's Law

One source of writhe is the tilting of the apex of a rising Ω-loop by the Coriolis force – Joy's Law. As it rises and expands a fluid parcel appears to rotate in a retrograde sense when viewed from the frame of the Sun. This causes the emerging sunspot pair to be tilted by an angle ψ, with the leading spot closer to the equator. Consider a flux tube which initially encircles the Sun in the Northern hemisphere (Figure 4). The rising and tilting gives the tube's axis a right handed pitch ($Wr > 0$) and thus a negative twist q in agreement with the tendency in Figure 1.

To calculate the writhe we begin with two limits in which Wr can be found readily. Without tilt ($\psi = 0$) the axis lies in a plane of constant latitude, even after rise, and therefore has $Wr = 0$. Alternatively, a tilt of $\psi = 180^\circ$ deforms the axis into a figure-eight for which $Wr = +1$ (Berger and Field 1984; Moffatt and Ricca 1992). We propose that intermediate values of tilt produce values of writhe $Wr \simeq \psi/180^\circ$.

During the period of rise, torsional Alfvén waves will equalize $q(\ell)$ over some axial length L, giving an estimate of

$$q \simeq -\frac{2\pi\, Wr}{L} \simeq -\frac{2\pi\, \psi}{180^\circ L} \quad , \tag{9}$$

at the apex. Since the rise speed is always less than $v_{\mathrm{A}\|}$, by Equation (2), we can deduce that $L > 200$ Mm, the depth of the CZ. For a typical active region tilt angle of $\psi = 6^\circ$ (Howard 1996) this gives an upper bound $|q| \lesssim 10^{-3}\,\mathrm{rad/Mm}$ on the amount of twist possible from Joy's law tilt. This is an order of magnitude smaller than observed, and cannot be the primary source of twist. (It is, however, comparable to the magnitude of the mean trend.) It should be further noted that this mechanism would lead to a correlation between observed values of q (i.e. α_{pcm}) and tilt ψ. This correlation has not been observed (Pevtsov 1999).

5.2. Differential Rotation

A second source of writhe is the well known differential rotation of the Sun. This process acts over extremely long times during which it is unlikley that a single flux tube could survive. By assuming the tube to survive indefintely, however, we can estimate the *maximum* twist possible; dissipation of the tube would presumably destroy its twist. Figure 5 shows the kind of tube typically presented in cartoons of the Babcock dynamo. A portion below the surface has been subjected to differential rotation while remaining connected through the corona. The "feet" of the tube are at different latitudes in the same hemisphere (more traditional cartoons have feet in opposite hemispheres; this would produce even less twist). After sufficient time the high-latitude foot has been "lapped" $N = 4$ times. The writhe of the resulting curve is $Wr \simeq N - \frac{1}{2}$. Thus each additional lap will add one to Wr while increasing the length L by $2\pi R_{\mathrm{CZ}} \cos(\theta)$, where $R_{\mathrm{CZ}} \simeq 500$ Mm is the radius of the CZ base. The process is slow enough for twist to equilibriate over the entire tube leading to $q \simeq 1/R_{\mathrm{CZ}} \simeq 2 \times 10^{-3}\,\mathrm{rad/Mm}$. This is well below observed values, and represents an upper bound on the twist possible from differential rotation.

5.3. The Σ-effect

The presence of two spatial derivatives (i.e. $\hat{\mathbf{l}} = \partial\mathbf{x}/\partial\ell$) in the definition of Wr (8) suggests that axis defomations on smaller scales may lead to more writhe than the large-scale mechanisms considered above. During its rise a tube will be buffeted by turbulent motions in the CZ. These motions are on the scale of the so-called mixing length, which decreases to several Mm towards the top of the CZ (Böhm-Vitense 1958; Spruit 1974). Moreover, the turbulent velocity is thought to have a helical nature characterized by its kinetic helicity $\langle \mathbf{u} \cdot \nabla \times \mathbf{u} \rangle$. For the bulk of the CZ this quantity is believed to be negative in the Northern hemisphere (Steenbeck and Krause 1966). Fluid motions with negative kinetic helicity generate right-handed deformations in a flux tube (Parker 1955b). These right-handed deformations will give rise to a positive writhe, and thus negative twist in the North. This sign is consistent with the trend in the data (Figure 1) and the random character of the turbulence might explain its large statistical dispersion. This turbulent mechanism of twist generation is known as the Σ-effect (Longcope *et al.* 1998).

The Σ-effect generates twist of the *same* sign as the kinetic helicity. This differs from the sign relationship in the traditional alpha-effect of mean-field dynamo theory: $\alpha \sim -\langle \mathbf{u} \cdot \nabla \times \mathbf{u} \rangle$. This discrepency arises because the α-effect concerns motions *internal* to a magnetic field, while the Σ-effect concerns motions *external* to the field (i.e. outside the flux tube). Consequenlty, when using motions in the bulk of the CZ, the Σ-effect agrees with the observed sense of twist while the α-effect does not.

The magnitude of the Σ-effect has been estimated by numerical simulation (Longcope *et al.* 1998). An initially untwisted, unwrithed flux tube was subjected to a random external velocity field representing the CZ turbulence. This velocity field had the amplitude, correlation length and kinetic helicity characteristic of mixing-length turbulence. The turbulence characteristics changed as the tube rose through the CZ. Equations for q and ω were solved until the end of the rise, yielding a single realization of q. To determine the statistical distribution of q, the procedure is then repeated 1000 times, each time with a different realization of the turbulent velocity. The distribution is then computed for tubes of different fluxes Φ at different solar latitudes. Figure 1 shows the mean (solid) and standard deviation (dashed) of the distribution for $\Phi = 10^{22}$ Mx. The typical values correspond to $q \sim 0.02$ rad/Mm, consistent with the data. Moreover, the latitudinal variations and level of statistical dispersion agrees remarkably well with observation.

5.4. Initial Twist

Finally, we turn to the possibility of twist in flux tubes *prior to their rise*. Present thinking holds that a dynamo operating at the base of the CZ generates a layer of smooth magnetic field which then fragments to form flux tubes (Cattaneo *et al.* 1990; Matthews *et al.* 1995). A mean-field α-Ω dynamo generates flux with some magnetic helicity (Charbonneau and Gilman 1998; Gilman and Charbonneau 1999). Present understanding of the fragmentation process, however, does not predict how this helicity might be converted to twist q_0 in the flux tubes which break free from the layer.

For the sake of a rough estimate we will consider the "twist" implied by the helicity in the dynamo layer itself, ignoring the fragmentation process entirely. An α-Ω dynamo produces magnetic fields and currents which are primarily torroidal. Magnitudes of these fields cannot be found from the standard linear treatments, however, their ratio can (Charbonneau and Gilman 1998). In particular an estimate of q_0 can be found,

$$q_0 \sim \frac{1}{2} \frac{\max \left(\nabla \times \mathbf{B} \right)_t}{\max B_t} \quad , \tag{10}$$

where maxima over space are found for the torroidal components of each field. This quantity is quite sensitive to model parameters such as α and the dynamo number. Parameter variations give values of q_0 ranging from 3×10^{-6} rad/Mm to 3×10^{-2} rad/Mm, with a reasonable choice yielding $q_0 \simeq 4 \times 10^{-5}$ rad/Mm (Charbonneau and Gilman 1998).

It is also possible that the poorly understood fragmentation process, which creates flux tube from the smooth dyanmo layer, introduces twist itself. It should be born in mind, however, that all of the mechansims mentioned in previous sections would add twist on top of q_0, present initially. The significant amount of twist contributed by the Σ-effect leaves little room in the observations for q_0.

6. Summary and Discussion

Observations indicate that solar magnetic flux tubes consist of twisted magnetic field. The magnitude and sign of the twist are measured by the quantity $\alpha_{\rm pcm}$, which shows a latitudinal variation in $\alpha_{\rm pcm}$ but with significant scatter. Table 1 lists the magnitude of observed twist along with theoretical predictions and constraints. Thin flux tube models show that large-scale sources, such as differential rotation or Joy's law, cannot explain the magnitude or latitudinal dependance of the observed twist. Turbulent buffeting of the rising tubes generates twist, through the Σ-effect, which does fit the observations, in magnitude, latitudinal dependance and degree of statistical dispersion.

A different category of comparison comes from application of two-dimensional MHD models to flux tubes. These predict minimum values of twist necessary for integrity or instability. Obsevations suggest that AR flux tubes remain in one piece during most of their rise from the base of the CZ. Almost none of the ARs observed, however, satisy the criterion for integrity (Equation [3]). This points to an inadequacy of the models or their interpretation. It has been suggested (Longcope *et al.* 1996; Emonet and Moreno-Insertis 1998) that the requirement for tube integrity in a fully three dimensional MHD model would be different than for the perfectly straight two-dimensional models used to derive Equation (3). Numerical simulations presently underway will help to clarify this point.

The threshold for helical kinking also stands well below the observed twist of ARs. While proper motion studies provide evidence of kinking, only a portion of any AR appears kinked. Until models are developed for complexes of interlinked flux tubes, however, it is not easy to appreciate the significance of this. There is at least one example in which the axis of an entire AR flux tube was observed to be kinked (Pevtsov and Longcope 1998), however, it is unclear if this is related to a helical kink instability.

Considerable uncertainty remains in the method of measuring the twist in an AR flux tube. The quantity $\alpha_{\rm pcm}$, developed by Pevtsov, Canfield and Metcalf [1995], has certain advantages over e.g. $\alpha_{\rm avg}$. Primary among these is the extensive dataset of ARs for which $\alpha_{\rm pcm}$ has been (laboriously) calculated. The technique itself should be studied in more detail to determine any biases it may introduce. More importantly, however, it must be determined how well any photospheric measurement can ascertain the twist which was present in the rising tube. In short, we must learn much more about the interface between CZ and the corona: the photosphere. Principally, does the photospheric twist reflect that in the rising tube, and does the photosphere influence the dytnamics of the tube?

We wish to thank Drs. Charbonneau and Gilman for performing the calculations in Section 5.4, and for contributions to the discussion therein.

References

Bao, S. and Zhang, H. (1998). *ApJ* **496**, L43.

Berger, M. A. and Field, G. B. (1984). *JFM* **147**, 133.

Böhm-Vitense, E. (1958). *ZAp* **46**, 108.

Caligari, P., Moreno-Insertis, F., and Schüssler, M. (1995). *ApJ* **441**, 886.

Cattaneo, F., Chiueh, T., and Hughes, D. (1990). *JFM* **219**, 1.

Charbonneau, P. and Gilman, P. (1998). Private communications.

Chou, D.-Y. and Fisher, G. H. (1989). *A&A* **341**, 533.

Choudhuri, A. R. and Gilman, P. A. (1987). *ApJ* **316**, 788.

Chui, A. Y. K. and Moffatt, H. K. (1995). *Proc. Roy. Soc. Lond.* **451**, 609.

D'Silva, S. and Choudhuri, A. R. (1993). *A&A* **272**, 621.

Emonet, T. and Moreno-Insertis, F. (1998). *ApJ* **492**, 804.

Fan, Y., Fisher, G. H., and McClymont, A. N. (1994). *ApJ* **436**, 907.

Fan, Y., Zweibel, E. G., Linton, M. G., and Fisher, G. H. (1998a). *ApJ* . In press.

Fan, Y.-H. and Fisher, G. H. (1996). *Solar Phys.* **166**, 17.

Fan, Y.-H., Zweibel, E. G., and Lantz, S. R. (1998b). *ApJ* **493**, 480.

Ferriz-Mas, A. and Schüssler, M. (1990). On the thin magnetic flux tube approximation. In Russel, C. T., Priest, E. R., and Lee, L. C., editors, *Physics of Magnetic Flux Ropes*, volume 58 of *Geophys. Monographs*, pp. 141–148. AGU.

Ferriz-Mas, A., Schüssler, M., and Anton, V. (1989). *A&A* **210**, 425.

Fisher, G. H., Fan, Y., and Howard, R. F. (1995). *ApJ* **438**, 463.

Gilman, P. and Charbonneau, P. (1999). Creationof twist at the core-convection-zone interface. In *This volume*.

Hood, A. W. and Priest, E. R. (1981). *Geophys. Astrophys. Fluid Dynamics* **17**, 297.

Howard, R. F. (1996). *Solar Phys.* **169**, 293.

Klapper, I. and Tabor, M. (1994). *J. Phys. A* **27**(14), 4919.

Krall, J., Chen, J., Santoro, R., Spicer, D. S., Zalesak, S. T., and Cargill, P. J. (1998). *ApJ* **500**, 992.

Leka, K. D., Canfield, R. C., McClymont, A. N., and Van Driel Gesztelyi, L. (1996). *ApJ* **462**, 547.

Linton, M. G., Dahlburg, R. B., Fisher, G. H., and Longcope, D. W. (1998a). *ApJ* **507**. in press.

Linton, M. G., Fisher, G. H., Dahlburg, R. B., Fan, Y.-H., and Longcope, D. W. (1998b). Multi-mode kink instability as a mecahnism for delta-spot fomation. In *Proceedings of the 1998 COSPAR meeting*. in press.

Linton, M. G., Longcope, D. W., and Fisher, G. H. (1996). *ApJ* **469**, 954.

Longcope, D. W. and Fisher, G. H. (1996). *ApJ* **458**, 380.

Longcope, D. W., Fisher, G. H., and Arendt, S. (1996). *ApJ* **464**, 999.

Longcope, D. W., Fisher, G. H., and Pevtsov, A. A. (1998). *ApJ* **507**. in press.

Longcope, D. W. and Klapper, I. (1997). *ApJ* **488**, 443.

Matthews, P., Hughes, D., and Proctor, M. (1995). *ApJ* **448**, 938.

Metcalf, T. R., Jiao, L., McClymont, A. N., Canfield, R. C., and Uitenbroek, H. (1995). *ApJ* **439**, 474.

Moffatt, H. K. and Ricca, R. L. (1992). *Proc. Roy Soc. Lond. A* **439**, 411.

Moreno-Insertis, F. (1983). *A&A* **122**, 241.

Parker, E. N. (1955a). *ApJ* **121**, 491.

Parker, E. N. (1955b). *ApJ* **122**, 293.

Parker, E. N. (1970). *ApJ* **162**, 665.

Parker, E. N. (1975). *ApJ* **198**, 205.

Parker, E. N. (1979). *Cosmical Magnetic Fields, Their Origin and Their Activity*. Clarendon Press, Oxford.

Pevtsov, A. A. (1999). Helicity of the photospheric magnetic field. In *This volume*.

Pevtsov, A. A., Canfield, R. C., and Metcalf, T. R. (1994). *ApJ* **425**, L117.

Pevtsov, A. A., Canfield, R. C., and Metcalf, T. R. (1995). *ApJ* **440**, L109.

Pevtsov, A. A. and Longcope, D. W. (1998). *ApJ* **508**. In press.

Priest, E. R. (1982). *Solar Magnetohydrodynamics*, volume 21. D. Reidel, Boston.

Rust, D. M. (1994). *Geophys. Res. Lett.* **21**, 241.

Schüssler, M. (1979). *A&A* **71**, 79.

Shafranov, V. D. (1957). *J. Nucl. Eng. II* **5**, 86.

Spruit, H. (1974). *Solar Phys.* **34**, 277.

Spruit, H. C. (1981). *A&A* **98**, 155.

Steenbeck, M. and Krause, F. (1966). *Z. Naturforsch* **21a**, 1285.

Tanaka, K. (1991). *Solar Phys.* **136**, 133.

Tsinganos, K. (1980). *ApJ* **239**, 746.

Turner, J. (1973). *Buoyancy Effects in Fluids.* Cambridge University Press.

Zhugzhda, Y. Y. (1996). *Physics of Plasmas* **3**(1), 10.

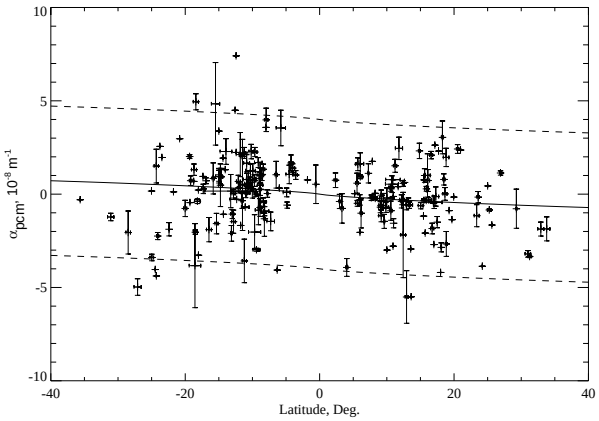

Fig. 1.— Values of $\alpha_{\rm pcm}$ measured in 203 ARs plotted against solar latitude. Error bars reflect variation in multiple measurements of the same AR. The solid line shows the mean value of $\alpha_{\rm pcm}$ generated by the theoretical Σ-effect in a flux tube of $\Phi = 10^{22}$ Mx. The intrinsic scatter in the Σ-effect is shown by the dashed lines.

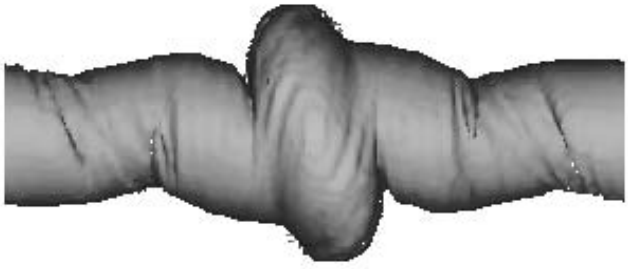

Fig. 2.— The saturated state of a helical kink instability. From nonlinear three-dimesnional simulations of Linton *et al.* [1998b]

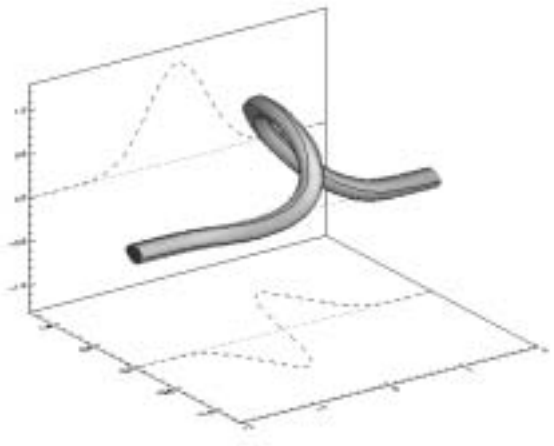

Fig. 3.— A flux tube (grey) on which several field lines are drawn. The axis of the tube has been deformed in a left-handed sense. The field lines twist about the axis to the right. The field lines at the ends of the tube have not moved during this deformation.

Fig. 4.— A flux tube tilted by the Coriolis force acting on the rising apex.

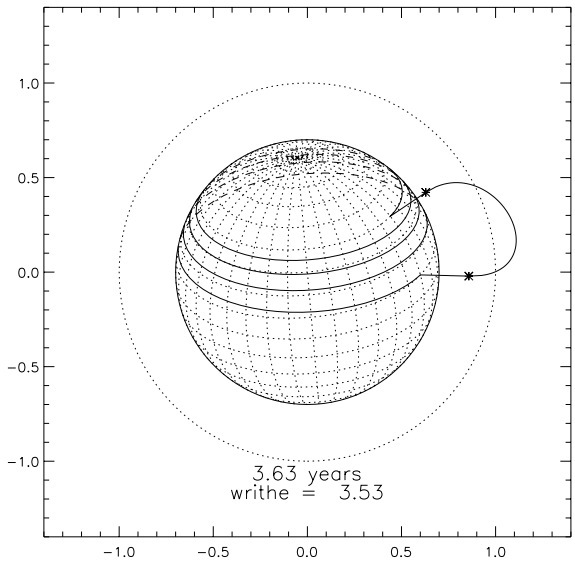

Fig. 5.— The axis of a flux tube, and its coronal connection, subjected to differential rotation.

	q (rad/Mm)	source	Ref.
Observations			
AR	~ 0.01	Fig. 1	a
substructures	~ 0.2	—	b, c
Constraints on twist			
Integrity of tube	$q \gtrsim 0.1$	Eq. (3)	d, e
Kink stable		Eq. (4)	f
overshoot	$q \lesssim 0.5$		
always	$q \lesssim 0.1$		
Sources of twist			
Joy's Law	0.001	Eq. (9)	g
Diff'l rotation	0.002	—	—
Σ-effect	~ 0.02	Fig. 1	h
Created in dynamo	4×10^{-5}	Eq. (10)	i

Table 1: A quantitative summary of twist q in flux tubes

[a] Pevtsov, Canfield and Metcalf 1995

[b] Pevtsov, Canfield and Metcalf 1994

[c] Leka *et al.* 1996

[d] Emonet and Moreno-Insertis 1998

[e] Fan, Zweibel and Lantz 1998

[f] Linton, Longcope and Fisher 1996

[g] Longcope and Klapper 1997

[h] Longcope, Fisher and Pevtsov 1998

[i] Charbonneau and Gilman 1998